

Article

Pore Water and Its Multiple Controlling Effects on Natural Gas Enrichment of the Quaternary Shale in Qaidam Basin, China

Xianglu Tang * , Zhenxue Jiang, Zhenglian Yuan, Yifan Jiao, Caihua Lin and Xiaoxue Liu 

State Key Laboratory of Petroleum Resources and Engineering, China University of Petroleum-Beijing, Beijing 102249, China; zhenxue_jiang@sina.com (Z.J.); yzl200996@163.com (Z.Y.); j247018642f@163.com (Y.J.); linch@student.cup.edu.cn (C.L.); iris_1314_iris@163.com (X.L.)

* Correspondence: tangxl@cup.edu.cn

Abstract: Quaternary shale gas resources are abundant in the world, but Quaternary shale contains a lot of pore water, which affects the enrichment of shale gas. At present, the controlling effect of pore water on gas enrichment in Quaternary shale is not clear. Taking the Quaternary shale of Qaidam Basin, China as an example, this paper systematically studies the characteristics of pore water in Quaternary shale through X-ray diffraction rock analysis, nuclear magnetic resonance, methane isothermal adsorption and other experiments, and reveals the controlling effect of pore water on shale gas enrichment. The results show that clay shale and silty shale are mainly developed in Quaternary shale. The clay shale is more hydrophilic, and water mainly exists in micropores and mesopores. Silty shale is less hydrophilic, and water mainly exists in mesopores and macropores. Pore water controls the formation of shale gas by the content of potassium and sodium ions, controls the adsorption of shale gas by occupying the adsorption point on the pore surface, controls the flow of shale gas by occupying the pore space, and controls the occurrence of shale gas by forming water film. Therefore, pore water has multiple controlling effects on shale gas enrichment. This achievement is significant in enriching shale gas geological theory and guide shale gas exploration.

Keywords: shale gas; pore water; natural gas; enrichment; Quaternary



Citation: Tang, X.; Jiang, Z.; Yuan, Z.; Jiao, Y.; Lin, C.; Liu, X. Pore Water and Its Multiple Controlling Effects on Natural Gas Enrichment of the Quaternary Shale in Qaidam Basin, China. *Energies* **2023**, *16*, 6170. <https://doi.org/10.3390/en16176170>

Academic Editor: Hossein Hamidi

Received: 19 July 2023

Revised: 14 August 2023

Accepted: 17 August 2023

Published: 25 August 2023



Copyright: © 2023 by the authors. Licensee MDPI, Basel, Switzerland. This article is an open access article distributed under the terms and conditions of the Creative Commons Attribution (CC BY) license (<https://creativecommons.org/licenses/by/4.0/>).

1. Introduction

The Quaternary is the most recent epoch in geological history, beginning at 2.6 Ma and continuing to the present day. It is also one of the best-preserved strata in the geological record, with less sediment loss and being generally unchanged by rock formation processes [1]. Quaternary sediments are generally recognized in the field as unconsolidated rock and are associated with geomorphic features that represent sedimentary processes. The sediments are usually rich in sand, silt, and mud, to centimeter thickness, representing a seasonal cycle [2]. Quaternary shale deposits are widely developed in the world. In addition to mountains, the world's land and oceans are covered by Quaternary sediments, especially in ancient lake basins and modern lakes with extremely thick mud shale deposits [3]. The widely developed Quaternary shale has the potential to produce methane in large quantities. The global underground natural methane emission is up to 576 Tg per year [4]. Therefore, the amount of methane trapped in shale during geological history should be very considerable, and shale has great potential to form natural gas through methanogenesis. For example, the natural gas generated in the Sanhu area of the Qaidam Basin has retained geological reserves of more than $15,000 \times 10^8 \text{ m}^3$ in the Quaternary strata. At present, biological gas reservoirs have been found in the Quaternary shale of the Qaidam Basin. For example, well TN18 has obtained industrial gas flow in the shale formation, and the daily gas is up to $2 \times 10^4 \text{ m}^3$ [5]. The development area of Quaternary shale in the Sanhu area of the Qaidam Basin is 25,000 km² with a thickness of more than 2000 m, which has a wide range of reservoir-forming material basis [6].

The Quaternary shale generally contain a large amount of water. Pore water is an important part in shale [7]. It is of great significance to study the properties and distribution of pore water in shale for shale gas exploration and development. Pore water in shale mainly comes from two aspects: firstly, it comes from the primary water in the deposition process, that is, the water trapped in the shale during the deposition process; and secondly, it comes from the infiltration of groundwater, that is, the water formed when groundwater enters the shale through the infiltration of shale [8]. The mixing of these two bodies of water forms pore water in the shale. The pore water in Quaternary shale is mainly primary water. Fan et al. (2023) consider that pore water can exist not only in shale minerals, but also in shale organic matter [9]. Pore water mainly exists in pores and fractures, and its occurrence state can be divided into two forms: free water and adsorbed water [10]. According to Li et al. (2020), there is a critical pore size in theory, and pores smaller than this pore size are completely filled with adsorbed water, with adsorbed water saturation of 100% and free water saturation of 0% [11]. The pore structure of shale plays an important role in the distribution and occurrence of pore water. The pore water storage capacity of shale with complex pore structure and small pore volume is low, and it is mainly adsorbed water. Shales with simple pore structure and large pore volume have higher pore water storage capacity, mainly dominated by free water. Pore water affects the occurrence of shale gas [12]. For shale with complex pore structure and small pore volume, the storage capacity of pore water is low, and the occurrence and release of shale gas are relatively hard. The higher the saturation of pore water, the more difficult it is for shale gas to occur and be released. Because the presence of pore water takes up pore space, it reduces the storage space for shale gas [13]. Researchers mainly studied pore water through nuclear magnetic resonance (NMR) and molecular dynamics simulation, and believed that pore water is an important fluid composition in shale, crowding out the adsorption site of shale gas, which is unfavorable to the occurrence of shale gas [14].

The effect of pore water on shale gas is an important research topic in the field of shale gas exploration. However, the distribution characteristics of pore water in Quaternary shale are still unclear, and the influence of pore water on shale gas generation, migration and enrichment is still unrevealed. The existence of these problems restricts the development process of Quaternary shale gas. Therefore, through the study of reservoir characteristics, pore water characteristics, pore water on methane generation, and the occurrence of Quaternary shale in the Qaidam Basin, the characteristics of pore water in Quaternary shale and its multiple controlling effects on natural gas enrichment are discussed in detail. This study provides a scientific basis for the efficient development of shale gas.

2. Geological Background

Located in the northeastern part of the Qinghai-Tibet Plateau, the Qaidam Basin is one of the largest inland basins in northwest China [15]. The Sanhu area is located in the eastern part of the Qaidam Basin and is one of the most important sedimentary areas of the basin [16]. The geological background of this area is complex, mainly composed of Quaternary mudstone and sandstone. This paper will introduce the characteristics of geological structure, sedimentary environment, and lithology.

The Qaidam Basin is a multiphase sedimentary basin with a complex geological background [17]. In geological history, the basin has undergone many tectonic movements and magmatic activities, resulting in complex geological structures and rich sedimentary rocks [18]. The strata in the basin are mainly divided into Precambrian, Cambrian, Ordovician, Silurian, Devonian, Permian, Jurassic, Cenozoic, and other strata from bottom to top [19]. Among them, the Quaternary is the latest formation in the Qaidam Basin, which is mainly composed of shale, sandstone and other rocks, and is one of the most important sedimentary layers in the basin (Figure 1).

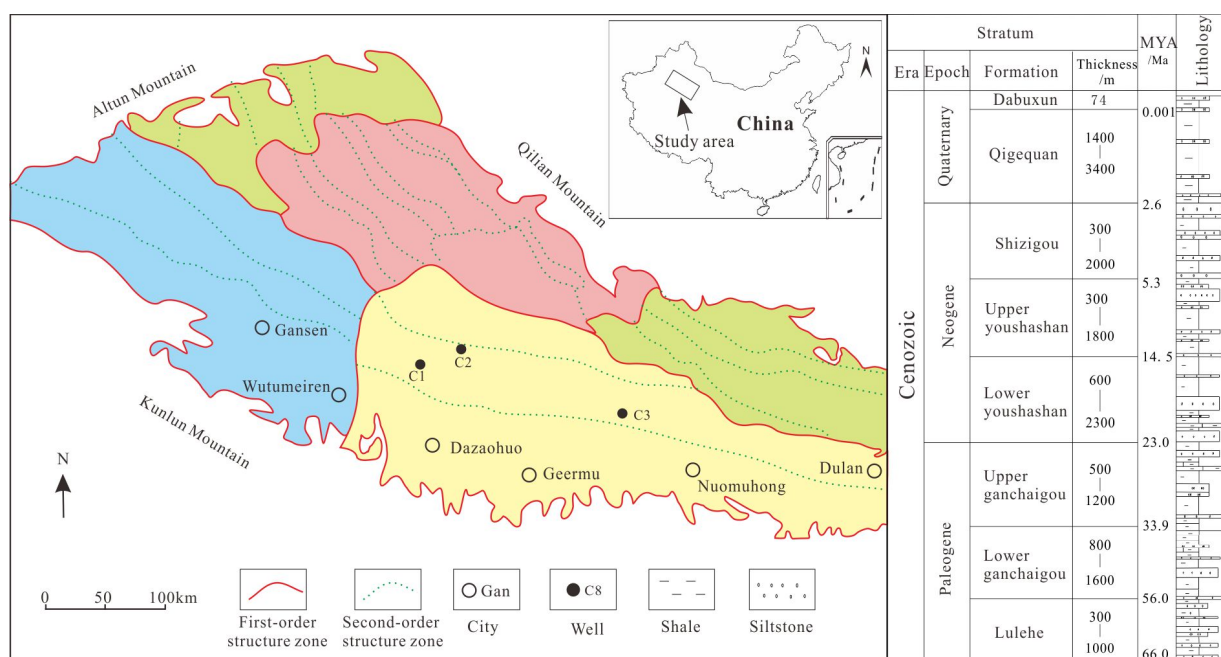


Figure 1. Structural characteristics and stratigraphic development characteristics of Qaidam Basin.

The sedimentary environment of the Quaternary shale is mainly affected by the basin structure and climate change [20]. Quaternary shale is mainly formed in the following periods. Late Quaternary: Climatic conditions were relatively wet, and the lake water body in the basin was relatively rich, which was one of the main environments for shale deposition [21]. Late Pleistocene: This period is another important sedimentary period of the Quaternary shale. At that time, the climatic conditions were relatively dry, the lake water body in the basin was gradually reduced, and the sedimentary environment of the shale gradually tended to be arid [22]. Holocene: The Holocene is the last sedimentary period of the Quaternary shale. At that time, the climatic conditions were relatively dry, the lake water in the basin almost disappeared, and the sedimentary environment of the shale was already tending to drought [23].

Shale, one of the most important sedimentary rocks of the Quaternary system, has the following characteristics. The color of the Quaternary shale is relatively simple, mainly gray, dark gray, yellow, and other colors [24]. The lithology of the Quaternary shale is diverse, including silty shale, clay shale, coal interlayer, etc., mainly silty shale and clay shale. The structure of the Quaternary shale is mainly stratified and jointed [25]. Among them, the bedding structure is more obvious, and the joint structures are relatively few. The mineral composition of Quaternary shale is mainly composed of quartz, feldspar, carbonate, clay, and other minerals. Among them, the content of quartz and clay is high, and they are the main components of the shale [26].

3. Materials and Methods

Silty shale and clay shale are two common rock types in the Quaternary shale of the Qaidam Basin. The physical properties and chemical compositions of these two types of rocks are different, which is significant for geological research and shale gas exploration and development. Therefore, this paper focuses on the selection of these two types of shale for analysis and testing. The samples are mainly taken from Wells C1, C2, and C3, as shown in Figure 1. Samples were collected from 30 clay shale (12 from Well C1, 9 from Well C2, and 9 from Well C3) and 35 silty shale (15 from Well C1, 12 from Well C2, and 8 from Well C3).

The organic matter (TOC) test was conducted using a high temperature combustion method [27]. The sample was burned at a high temperature to convert organic matter

into CO₂, and then the content of CO₂ was determined using an infrared spectrometer, and then the content of organic matter in the sample was calculated. The sample should be pulverized into a uniform fine powder to facilitate combustion at high temperatures. Inorganic carbon in the sample can interfere with the results of the TOC determination, so this needs to be removed. The removal method of inorganic carbon is to put the sample into a hydrochloric acid solution prepared with hydrochloric acid and distilled water at 1:7, and heat it in a water bath at 80 °C for more than 2 h until the reaction is complete. The TOC was tested using the TOC-4200 analyzer. The rock mineral was analyzed using a D2 PHASER X-ray diffractometer, the sample was crushed and ground to less than 40 µm particle size, the back-pressure method was used to form a tablet, and the 3–45° diffraction spectrum was obtained using the machine [28]. According to the corresponding formula in the standard and the mineral K value, various mineral content data were calculated. Using a DX-CP helium porosimeter to determine the porosity of the sample, the principle of which is according to the change in pressure and volume in Boyle's law, calculate the pore volume [29]. Using the TC-70 porous permeability meter to determine the overburden permeability, the principle of which is according to the Darcy's Law of seepage, determine the pressure difference and gas flow at both ends of the rock sample, using the Darcy formula to calculate the rock sample permeability. The concentration of ions in the shale formation water was measured using a 3400-AAS flame atomic absorption spectrometer. The water in the sample was distilled using the Dean–Stark method, and then the water saturation of the sample was calculated according to the water content and the sample porosity.

The contact angle test requires the preparation of a flat surface from the shale sample [30]. The shale sample is usually treated with a cutting machine to ensure that the sample surface is flat and there are no obvious bumps and cracks. The water was chosen as the experimental liquid. The prepared shale sample was placed on the experimental table. Then a drop of water was put on the shale surface. The contact angle measuring instrument was used to measure the contact angle of the drop water. For the nuclear magnetic resonance experiments, the sample was saturated with water to obtain different water saturation [31]. Then, the sample was put into the NMR instrument to obtain the NMR signals of the samples with different water saturation and analyze the distribution characteristics of water in shale. The samples with different water saturation were put into the methane isothermal adsorption instrument, and the temperature and pressure of the test were set to obtain the methane isothermal adsorption curves of the samples with different water saturations [32].

4. Results

4.1. Basic Characteristics of Shale

4.1.1. Lithology Characteristics

The Quaternary strata in the Qaidam Basin are mainly composed of shale and sandstone. The sandstone mainly exists in the shale as an interlayer with a thin thickness, but it is very common and widely developed. The Quaternary shale is mainly composed of clay shale and silty shale (Figure 2). Clay shale and silty shale have extremely strong vertical and lateral heterogeneity.

Clay shale mainly reflects underwater deposits and can be subdivided into a deep argillaceous layer and shallow argillaceous layer according to water depth. The deep argillaceous layer is mainly unstratified or hidden stratified, and is formed in a semi-deep lake environment under the wave base plane [33]. It is mainly composed of clay minerals dominated by illite, and the content can be as high as 80%. The shallow argillaceous layer is formed in the coastal shallow lake or coastal delta plain environment, which is generally unstratified or the stratification is modified, or the stratification is not significant [34]. It is mainly composed of clay minerals and micrite calcite, and is rich in plant roots and the shells of snails and ostracods.

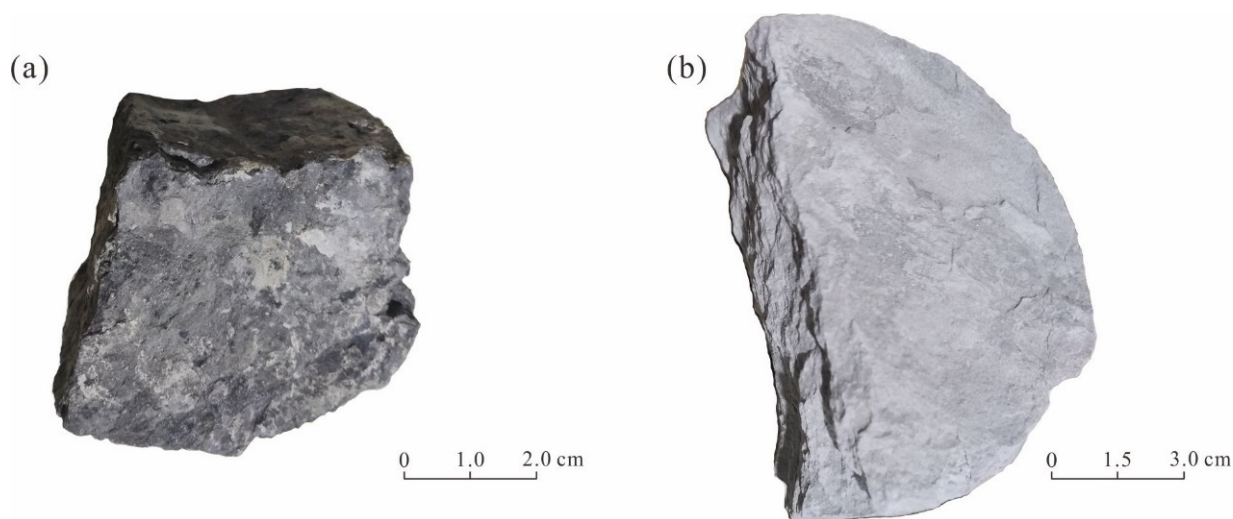


Figure 2. Features of the Quaternary shale in Qaidam Basin. (a) is clay shale, (b) is silty shale.

According to the composition and sedimentary structure characteristics, silty shale can be divided into two categories: seasonal laminae and scour laminae. Seasonal laminae and scour laminae are the reflection of glacial and interglacial periods [35]. The seasonal laminae include a stable interlayer formed by mud and silt, and an interlayer formed by organic mud and silt. The interlayer is generally 0.7~0.8 mm thick, of which the mud is generally about 0.5 mm, and the silt is usually about 0.1 mm. Scour laminae is also composed of mud and silt, there is the same period of erosion and transformation, and the silt layer and mud layer thicknesses are similar.

4.1.2. Reservoir Characteristics

The porosity of the Quaternary shale in the Qaidam Basin is generally higher than 10%, which is significantly higher than that of typical shale oil and gas reservoirs, and even more than 10 times that of the shale in the Qiongzhusi Formation in the Sichuan Basin [36]. Therefore, the reservoir space of Quaternary shale is extremely high, which provides very favorable conditions for natural gas accumulation. The porosity of clay shale and silty shale is also different, among which clay shale has the smallest porosity, with a peak value between 12% and 18%. Silty shale has the highest porosity, with peaks ranging from 16% to 25% (Table 1). The water saturation of Quaternary shale is generally high, among which the water saturation of clay shale ranges from 40 to 76% and that of silty shale ranges from 57 to 90%. The difference of organic matter content between clay shale and silty shale is also large. The TOC content of clay shale is relatively high, ranging from 0.5% to 1.5%. The TOC content of silty shale ranges from 0.3% to 0.8%. The mineral composition of Quaternary shale is mainly quartz and clay minerals, followed by carbonate minerals and feldspar. The clay mineral content in clay shale is the highest, ranging from 35% to 58%. Silty shale has the highest quartz content, ranging from 32% to 49%.

Table 1. Characteristics of Quaternary shale reservoirs in Qaidam Basin.

Lithology	Porosity (%)	Water Saturation (%)	TOC (%)	Mineral Composition (%)			
				Quartz	Feldspar	Carbonate Minerals	Clay Minerals
Clay shale	12–18	40–76	0.5–1.5	15–24	5–17	7–21	35–58
Silty shale	16–25	57–90	0.3–0.8	32–49	7–22	8–24	13–35

4.2. Pore Water Characteristics

4.2.1. Wettability Characteristics of Pore Water on Shale Surface

Because of the particularity of its microstructure, the wettability of shale shows some unique characteristics. Wettability refers to the distribution of the liquid on the solid surface, and the more evenly the liquid is distributed on the solid surface, the better the wettability [37]. For shale, its microstructure is mainly composed of quartz, feldspar, mica, and other minerals, and the surface of these minerals has certain chemical properties and structural characteristics, which affects the wettability of shale. The water contact angle refers to the angle between the contact line formed when the liquid is in contact with the solid and the solid surface [38]. The wettability of the shale surface can be judged by the size and variation of the contact angle.

It can be seen from the experiment of water contact angle of clay shale and silty shale that the initial contact angle of clay shale is small, only 27.5° . With the passage of time, the contact angle decreases rapidly, and the water spreads on the surface of the shale. After 2.5 s, the water is fully wetted to the interior of the shale, indicating that the water of the clay shale is extremely wettable (Figure 3). Silty shale has a relatively large initial contact angle of 40.3° . The contact angle also changes at a slower rate over time. Water spreads slowly over the shale surface. After 5 s, the contact angle of the water stabilizes and the water does not fully wet into the shale, indicating that the silty shale is relatively weak in water wettability (Figure 4). The main reason for the difference in wettability between clay shale and silty shale is their different mineral composition. Clay mineral content is higher in clay shale. Clay minerals have a certain hydrophilicity, and the oxygen atoms on the surface form a strong hydrogen bond with water molecules, so that the water molecules form a small contact angle on the clay surface [39]. The content of quartz minerals is high in silty shale. The quartz surface has a high surface energy, which causes water to form a large contact angle on the quartz surface.

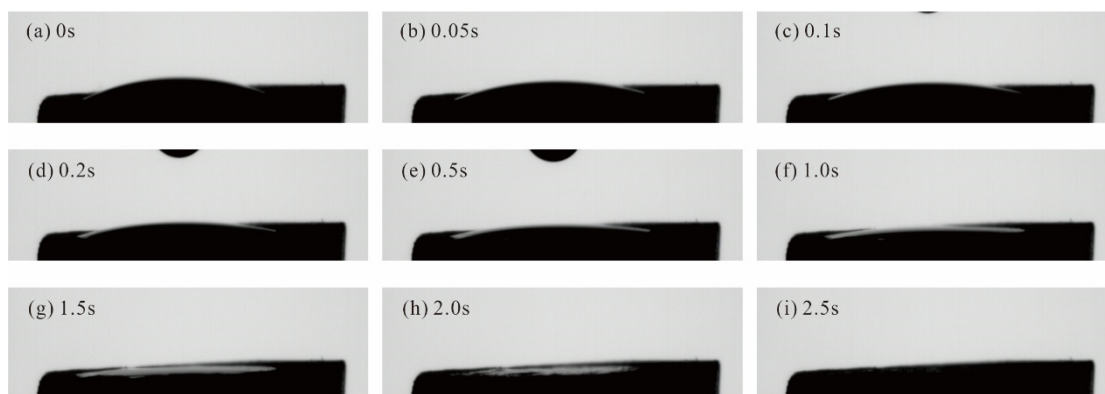


Figure 3. Variation characteristics of water contact angle in clay shale. The contact angle of water changes rapidly. At 2.5 s, the water has been completely wetted into the shale.

4.2.2. Distribution Characteristics of Pore Water in Shale

The distribution characteristics of pore water in Quaternary shale in the Qaidam Basin can be obtained through NMR experiments. In the Quaternary shale of the Qaidam Basin, pore water is usually stored in pores and fractures of different sizes, and the size and shape of these pores and fractures will affect the distribution characteristics of pore water [40]. Generally speaking, the distribution of pore water in the Quaternary shale in this basin can be divided into three categories: macropore water, mesopore water, and micropore water. Macropore water is usually distributed in the larger pores and fractures in the shales, and its T_2 spectrum peaks are between tens of milliseconds and hundreds of milliseconds. Mesopore water is usually tens of milliseconds. Micropore water is typically distributed in tiny pores and fractures in shale, with T_2 spectrum peaks ranging from a few milliseconds to tens of milliseconds.

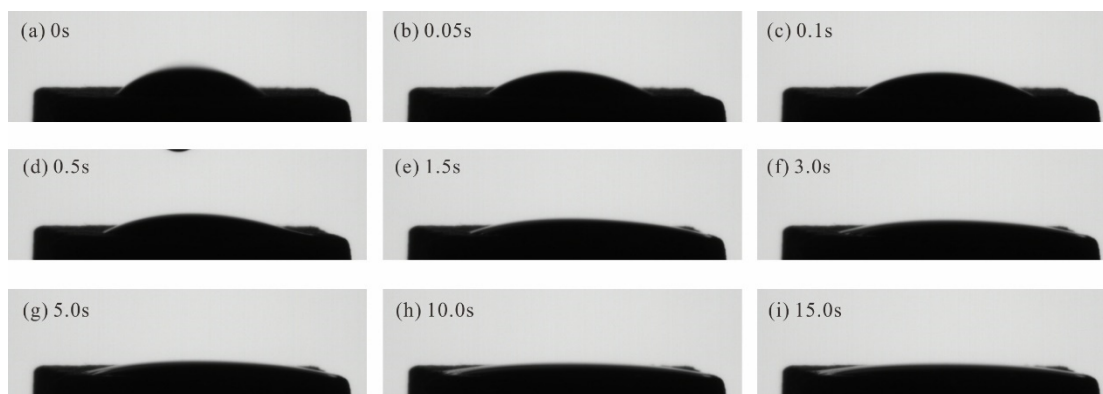


Figure 4. Variation of water contact angle in silty shale. The contact angle of water changes slowly. The water contact angle tends to stabilize after 5 s.

Clay shale and silty shale are the two most common rock types in Quaternary shale, and there are some differences in their physical properties and geological characteristics, including the NMR T_2 spectrum. Firstly, there are obvious differences in the pore structure of clay shale and silty shale. The pores in clay shale are usually small, irregular in shape, densely distributed, and have poor connectivity among them. On the other hand, the pores in silty shale are usually large, regular in shape, dispersed in distribution, and often connected with each other. Secondly, there are differences in the peak positions of NMR T_2 spectra between clay shale and silty shale. The peak value of the T_2 spectrum of pore water in clay shale is usually between a few milliseconds and tens of milliseconds, which is due to the irregular size and shape of pores in clay shale and poor connectivity between pores, which limits the movement of pore water (Figure 5). However, the peak value of the T_2 spectrum of pore water in silty shale is usually between a few milliseconds and several hundred milliseconds, which is due to the variable size and morphology of pores in silty shale and the interconnection between pores, so that the movement of pore water is relatively limited (Figure 6). In addition, there are differences in pore water distribution characteristics between clay shale and silty shale. The pore water in clay shale is usually distributed in the pores and fractures of different sizes, and the size and shape of these pores and fractures will affect the distribution characteristics of pore water [41]. The pore water in silty shale is usually distributed in the pores between the silty sand particles, and the size and shape of these pores will also affect the distribution characteristics of pore water. Therefore, the NMR T_2 spectra of clay shale and silty shale are different due to their different pore structures, pore water distribution characteristics, and the degree of restriction of pore water movement.

With the decrease in water saturation, pore water changes in nano-pores. Firstly, at high water saturation, pore water is usually distributed in pores of various sizes, including micropores, mesopores, and macropores. When the water saturation is reduced, pore water will be drained from the macropores and gradually distributed into micropores and mesopores. However, at very low water saturation, pore water can only be distributed in micropores (Figures 5 and 6). Secondly, when the water saturation is reduced, the interaction between pore water molecules is enhanced, so the movement of pore water molecules is restricted. In nanopores, the movement of pore water molecules is restricted even more significantly because the pore size is similar to the size of the pore water molecules. At this point, both the diffusion coefficient and the motion velocity of the pore water molecules are reduced. Thirdly, the surface tension of pore water increases with the decrease in water saturation. In nanopores, an increase in surface tension causes pore water molecules to gather near the pore wall, forming an adsorption layer [42]. This further restricts the movement of the pore water molecules and affects the interaction between the pore water and the pore wall.

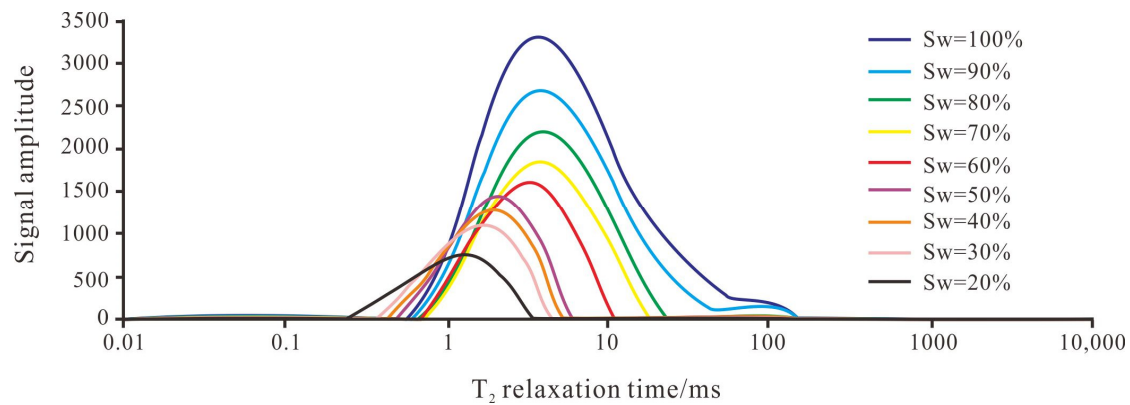


Figure 5. NMR characteristics of clay shale under different water saturation conditions. T_2 spectral peaks usually range from a few milliseconds to tens of milliseconds. As the water content increases, the T_2 spectrum peak gradually decreases.

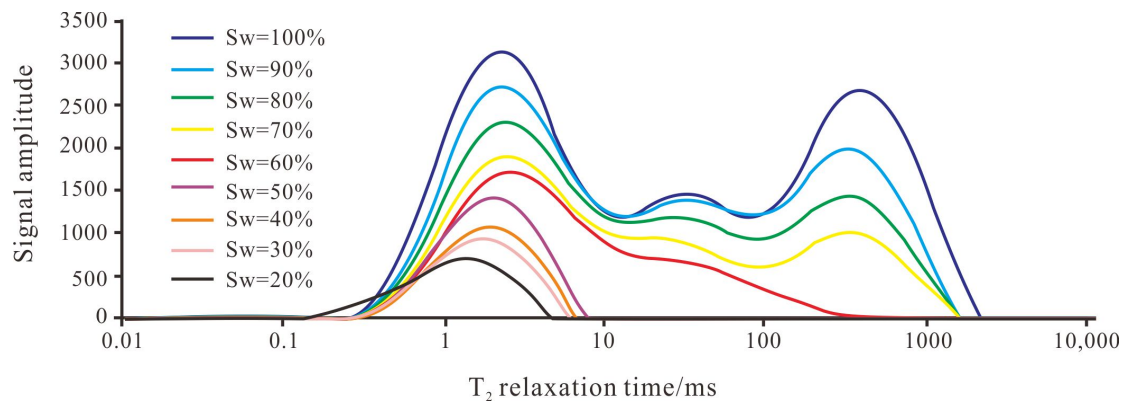


Figure 6. NMR characteristics of silty shale under different water saturation conditions. The peak value of the T_2 spectrum is usually between a few milliseconds and a few hundred milliseconds. As the water content increases, the T_2 spectrum peak gradually decreases.

5. Discussion

5.1. Effect of Pore Water on Natural Gas Generation

Shale is a sedimentary rock rich in organic matter, which can undergo a biogas formation reaction under appropriate conditions to produce methane, ethane, and other biogas. Pore water is a kind of water body in shale, and its influence on biogas generation in shale is very important. Pore water can be used as a reaction medium to promote biogas formation in shale [43]. The biogas formation reaction refers to the process of decomposition and recombination of organic matter molecules to produce methane, ethane, and other biogas under appropriate temperature, pressure, and microbial action. Pore water contains a variety of ions, including sodium, magnesium, calcium, potassium, chlorine, sulfate, bicarbonate, etc. (Table 2). These ions have different effects on biogas formation. Firstly, sodium ion is one of the most abundant ions in groundwater, and it is also one of the important components in the biogas formation process. In the process of producing biogas, organic matter will be degraded by anaerobic microorganisms, producing a large number of isobutane, ethane, methane, and other gases. In this process, sodium ion may play a catalytic role in promoting the speed and effect of organic matter degradation. Secondly, chloride ion is also a kind of ion with a high content in groundwater, and its influence on biogas generation is relatively weak [44]. The content of potassium and sodium ions in clay shale is higher than that in silty shale, so it has a stronger gas generation capacity.

Table 2. Ion content in pore water of Quaternary shale in Qaidam Basin.

Lithology	K ⁺ + Na ⁺ (mg/L)	Ca ²⁺ (mg/L)	Mg ²⁺ (mg/L)	CL ⁻ (mg/L)	SO ₄ ²⁻ (mg/L)	HCO ₃ ⁻ (mg/L)	Total Mineralization (mg/L)
Clay shale	57,145–66,317	2839–3249	497–2661	100,015–110,471	429–11,445	942–1131	164,101–182,922
Silty shale	36,906–55,074	2129–2657	861–1233	63,853–90,425	309–1311	660–942	106,620–149,740

In addition, the pore water also contains microorganisms, enzymes, and other bioactive substances; these substances can promote the decomposition of organic matter and the biogas generation reaction [45]. Secondly, pore water can affect the rate and yield of biogas generation in shale. The ions and molecules in pore water can affect the decomposition and recombination rate of organic matter molecules and the product distribution, thus affecting the rate and yield of biogas generation. In addition, physical conditions such as temperature and pressure in pore water can also affect the rate and yield of biogas generation. In summary, pore water has many effects on biogas matter molecules, and affects the rate and yield of biogas generation. Therefore, the role of pore water must be fully considered when studying the process and mechanism of biogas generation in shale.

5.2. Effect of Pore Water on Natural Gas Occurrence

Pore water forms a water film on the pore surface, which is usually from a few nanometers to tens of nanometers in thickness. The thickness of the pore water film is related to factors such as porosity and rock particles [46]. The calculation of water film thickness in pores involves concepts such as capillary pressure, formation pressure, and separation pressure (Figure 7). The water film thickness decreases with the increase in formation pressure, showing a negative correlation trend. This is because the increase in formation pressure will compress the water molecules in the pores, making their distribution more dense, thus reducing the thickness of the water film [47]. The water film thickness presents a nonlinear trend with the increase in formation pressure, that is, the change rate of water film thickness gradually slows down. This is because when the formation pressure is small, the water molecules in the pores are subjected to relatively small compression, and the water film thickness changes rapidly. However, with the increase in formation pressure, the water molecules in the pores are gradually saturated by compression, and the change rate of water film thickness gradually slows down.

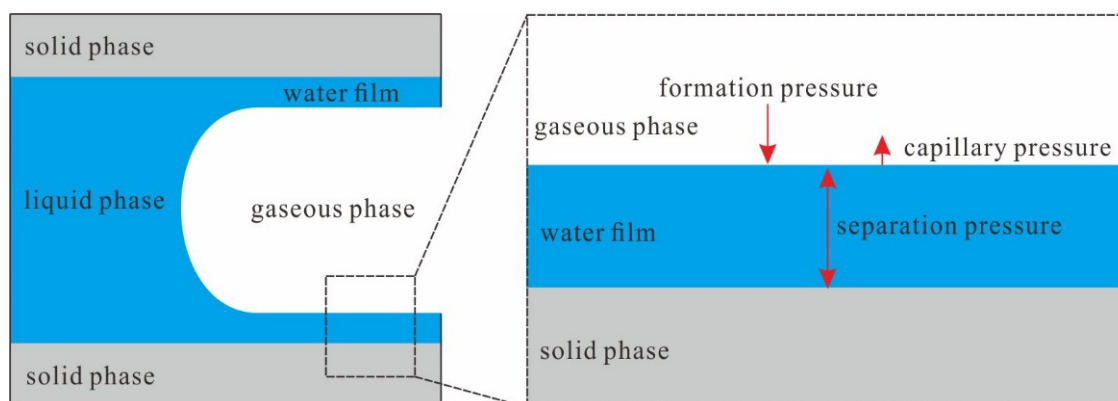


Figure 7. The force on the water film of Quaternary shale in Qaidam Basin. The water film thickness is affected by capillary pressure, formation pressure, and separation pressure.

It is assumed that the clay shale has a density of 2.0 t/m³ and a porosity of 15%, and the silty shale has a density of 2.5 t/m³ and a porosity of 20%. Porosity and density are

constant during the burial depth process. The change in free gas content can be calculated according to the following formula:

$$Q_{\text{free}} = (\varphi \cdot (1 - S_w) \cdot P_i \cdot T_0) / (\rho \cdot P_0 \cdot T_i) \quad (1)$$

where Q_{free} is free gas content, m^3/t ; φ is porosity, %; S_w is water saturation, %; ρ is the density, t/m^3 ; T_0 is the standard temperature, 273.15 K; P_0 is the standard pressure, 101.325 KPa; T_i is the temperature of the shale in the ground, K; and P_i is the pressure of the shale in the ground, Kpa.

The Quaternary shale in the Sanhu area is in the early diagenetic stage, and the average reservoir water saturation is between 40 and 90%, which is much higher than the shale gas area in North America and South China [48]. When the water saturation increases, the available gas reservoir space decreases, and the free gas volume also decreases. At the depth of 1800 m, when the water saturation reaches 80%, the theoretical free gas of clay shale can reach $2.22 \text{ m}^3/\text{t}$, and that of silty shale can reach $2.38 \text{ m}^3/\text{t}$ (Figure 8). Therefore, water in shale will affect the effective porosity and further reduce the occurrence space of free gas.

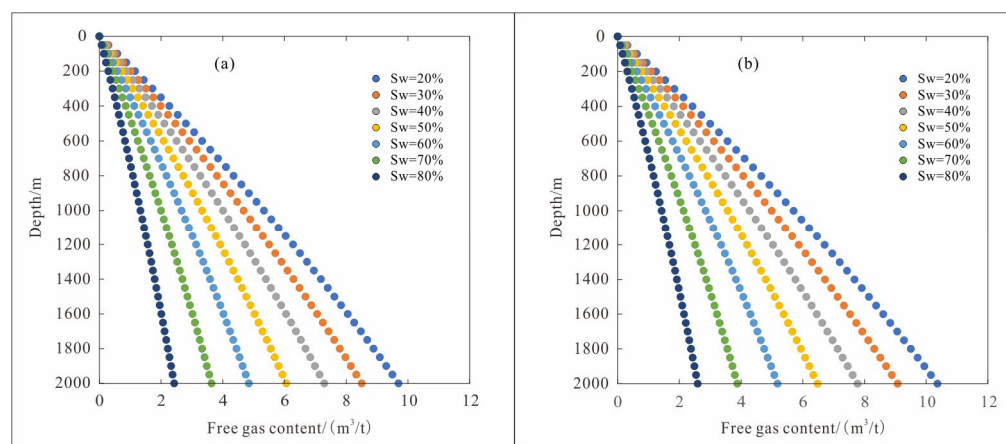


Figure 8. Variation trend of free gas in shale with different water saturation with depth. (a) is clay shale, (b) is silty shale. With the increase in burial depth, the free gas volume increases gradually. With the increase in water saturation, the free gas content decreases gradually.

5.3. Effect of Pore Water on Natural Gas Adsorption

The difference of methane isothermal adsorption in clay shale and silty shale is related to the pore structure of the reservoir. The pores in clay shale are mainly micropores and mesopores, while those in silty shale are mainly mesopores and macropores. The pore size of micropores and mesopores is smaller, so the pore structure of clay shale is more complex than that of silty shale and can provide more adsorption surface area, so the methane isothermal adsorption capacity of clay shale is usually higher than that of silty shale (Figure 9). In addition, the content of organic matter in clay shale is usually higher than that in silty shale, and organic matter is a major source of natural gas, thus increasing the isothermal adsorption of methane in clay shale [49]. However, this also means that the methane release rate in clay shale is slower, because the organic matter needs to be heated and under pressure to release the natural gas.

An increase in water saturation will lead to a decrease in porosity in the shale pores. This is because water molecules are larger in volume than methane molecules, and water molecules will occupy part of the pore space, limiting the entry of methane molecules into the pores. In addition, increased water saturation also leads to an increase in the wettability of the pore wall surface, which reduces the adsorption capacity of methane molecules on the pore wall surface [50]. Methane molecules and water molecules have the characteristics of competitive adsorption on quartz, clay minerals, and other components in shale. Clay

minerals and brittle minerals (quartz, feldspar, etc.) have adsorption capacity on the surface, and can adsorb methane molecules and water molecules. However, the adsorption capacity of clay mineral surfaces is generally higher than that of brittle mineral surfaces because clay mineral surfaces have more adsorption sites and richer surface chemical functional groups. Methane molecules and water molecules have different adsorption affinities on clay minerals and brittle mineral surfaces. In general, water molecules have a higher adsorption affinity than methane molecules because water molecules have stronger polarity and hydrogen bonding and can bind more tightly to mineral surfaces. When water and methane molecules are present at the same time on the mineral's surface, they engage in competitive adsorption. In general, water molecules will adsorb preferentially because they have a higher adsorption affinity and stronger polarity [51]. This competitive effect results in lower adsorption of methane molecules, which affects the storage and migration of natural gas in the reservoir. In addition, temperature also has an effect on the adsorption characteristics of methane and water molecules on the surface of clay minerals and brittle minerals. In general, as the temperature increases, the amount of methane and water molecules adsorbed on the surface of minerals decreases. However, different mineral surfaces respond differently to temperature, which can also affect competitive adsorption characteristics.

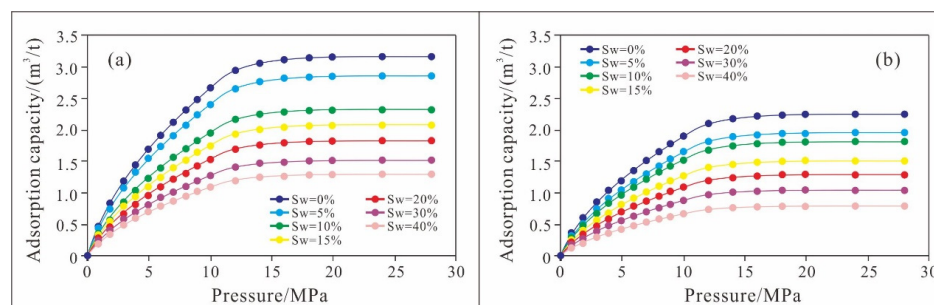


Figure 9. Isothermal adsorption curves of methane in shales with different water saturation. (a) is clay shale with large adsorption capacity. (b) is silty shale with small adsorption capacity.

The amount of methane adsorption in the Quaternary shale in the Qaidam Basin is related to the amount of water molecules adsorbed on the pore surface, because water molecules will occupy part of the pore surface, thus affecting the amount of methane molecules adsorbed on the pore surface. Therefore, there is a certain correlation between water saturation and the maximum adsorption amount of methane. In order to predict in situ methane adsorption in real formation, it is necessary to construct a correlation curve between water saturation and maximum methane adsorption. This curve can be obtained by laboratory measurement and data fitting. Based on the methane adsorption capacity and water saturation of clay shale and silty shale samples measured in the laboratory at a certain temperature and pressure, the relationship between water saturation and the maximum methane adsorption capacity can be obtained (Figure 10). According to the correlation curve between water saturation and maximum methane adsorption, it is predicted that the methane adsorption capacity of the Quaternary shale in the Qaidam Basin is only $0.49 \text{ m}^3/\text{t}$, and that of the silty shale is only $0.27 \text{ m}^3/\text{t}$ when the water content is 80%. Therefore, the methane adsorption capacity of shale will be significantly reduced with water content.

5.4. Effect of Pore Water on Natural Gas Flow

Pore water content has great influence on methane transport. A pore is a small space inside the rock; due to its small size, physical adsorption, capillary action and chemical adsorption, and other effects, this will lead to a certain amount of water in the pore [52]. The presence of pore water can change the porosity and permeability of the rock, thus affecting the flow of methane. Firstly, there is a microscopic interaction between pore water content and shale permeability. In shale, pore water is a fluid that fills tiny pores, creating a

kind of nanoscale interfacial region between the pores and the rock particles. Therefore, changes in pore water content directly affect the number, size, and connectivity of these very small channels, and thus directly determine the shale permeability (Figure 11). At the molecular scale, the effect of pore water content on shale permeability depends on the pore structure and the interaction of water molecules with the rock surface [53]. When the pore water content increases, the flow of water molecules in the pores is constrained, and the interaction between water molecules and the rock surface is also enhanced, thus reducing the permeability. In addition, water molecules may also reduce permeability by filling the pores and reducing the presence of gas.

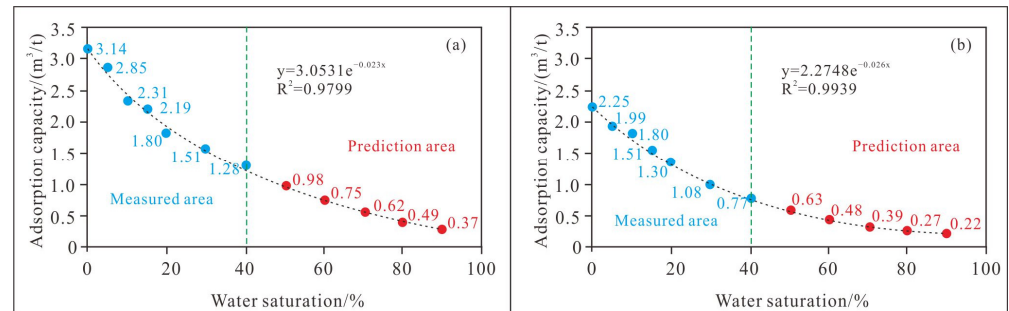


Figure 10. Variation trend of adsorbed gas of shale with different water saturation. (a) is clay shale, (b) is silty shale. With the increase in water saturation, methane adsorption decreases gradually. The methane adsorption capacity of clay shale is higher than that of silty shale.

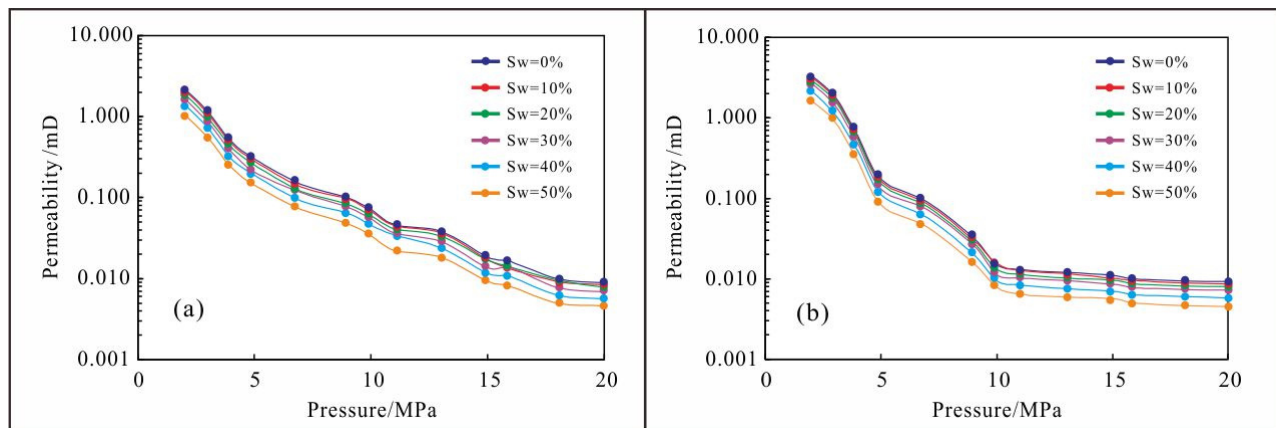


Figure 11. Variation characteristics of overburden permeability of shale with different water saturation. (a) is clay shale, (b) is silty shale. With the increase in water saturation, the permeability of shale decreases gradually. As the pressure increases, the permeability of the shale gradually decreases.

6. Conclusions

(1) The Quaternary shale mainly develops clay shale and silty shale, which provide very favorable conditions for natural gas accumulation. Clay shale has relatively low porosity (12–18%), high TOC content (0.5–1.5%), low water saturation (40–76%), and high clay mineral content (35–58%). Silty shale has relatively high porosity (16 to 25%), low TOC content (0.3 to 0.8%), high water saturation (57 to 90%), and high quartz content (32% to 49%).

(2) The initial contact angle of clay shale is small, only 27.5°. As time goes on, the contact angle decreases rapidly, and water spreads out on the surface of the shale, making it extremely wettable. Silty shale has a relatively large initial contact angle of 40.3°. The contact angle also changes more slowly over time and is relatively weak in water wettability. The peak of the T₂ spectrum of pore water in clay shale usually ranges from a few milliseconds to tens of milliseconds. The peak T₂ spectrum of pore water in silty shales

usually ranges from a few milliseconds to a few hundred milliseconds. With the decrease in water saturation, pore water changes in nano-pores. The pore water will be discharged from the macropores and gradually distributed into micropores and mesopores.

(3) Shale pore water contains a variety of ions; potassium and sodium ions are some of the ions with the highest content in pore water, and they are also some of the important components in the process of natural gas generation, playing a catalytic role in promoting the speed and effects of organic matter degradation. Pore water content also affects the adsorption amount of natural gas. With the increase in water content, methane adsorption capacity decreases. The pore water content has great influence on methane flow. With the increase in water content, the physical property of shale deteriorates, and the migration capacity of methane also decreases. Pore water in shale forms a water film on the pore surface, which affects the effective porosity of shale and further reduces the occurrence space of free gas.

Author Contributions: Conceptualization, X.T.; methodology, Z.J.; software, Z.Y.; validation, Y.J., X.T. and Z.J.; formal analysis, C.L.; investigation, X.L.; resources, Z.J.; data curation, X.T.; writing—original draft preparation, X.T.; writing—review and editing, Z.J. and X.L.; visualization, Z.Y.; supervision, Y.J.; project administration, X.T.; funding acquisition, C.L. All authors have read and agreed to the published version of the manuscript.

Funding: This research was funded by The National Natural Science Foundation of China, grant number 41802153.

Data Availability Statement: Data are available from the authors upon reasonable request.

Acknowledgments: We acknowledge the support received from the China National Petroleum Corporation. We express our appreciation for their provision of experimental samples.

Conflicts of Interest: The authors declare no conflict of interest.

References

1. Land, L.S.; Mack, L.E.; Milliken, K.L.; Leo Lynch, F. Burial diagenesis of argillaceous sediment, south Texas Gulf of Mexico sedimentary basin: A reexamination. *Geol. Soc. Am. Bull.* **1997**, *109*, 2–15. [[CrossRef](#)]
2. Rigsby, C.A.; Bradbury, J.P.; Baker, P.A.; Rollins, S.M.; Warren, M.R. Late Quaternary palaeolakes, rivers, and wetlands on the Bolivian Altiplano and their palaeoclimatic implications. *J. Quat. Sci.* **2005**, *20*, 671–691. [[CrossRef](#)]
3. Liu, Z.; Wang, Y.; Chen, Y.; Li, X.; Li, Q. Magnetostratigraphy and sedimentologically derived geochronology of the Quaternary lacustrine deposits of a 3000 m thick sequence in the central Qaidam basin, western China. *Palaeogeogr. Palaeoclimatol. Palaeoecol.* **1998**, *140*, 459–473.
4. Saunois, M.; Staver, A.R.; Poulter, B.; Bousquet, P.; Canadell, J.G.; Jackson, R.B.; Raymond, P.A.; Dlugokencky, E.J.; Houweling, S.; Patra, P.K.; et al. The global methane budget 2000–2017. *Earth Syst. Sci. Data* **2020**, *12*, 1561–1623. [[CrossRef](#)]
5. Shao, Z.; He, S.; Hou, L.; Wang, Y.; Tian, C.; Liu, X.; Zhou, Y.; Hao, M.; Lin, C. Dynamic accumulation of the Quaternary shale biogas in Sanhu Area of the Qaidam Basin, China. *Energies* **2022**, *15*, 4593. [[CrossRef](#)]
6. Hui, Y.; Zhang, Y.; Dade, M.; Baihong, W.; Shiyong, Y.; Ziyuan, X.; Xiaoping, Q. Integrated geophysical studies on the distribution of Quaternary biogenic gases in the Qaidam Basin, NW China. *Adv. Pet. Explor. Dev.* **2012**, *39*, 33–42.
7. Tian, H.; Wang, M.; Liu, S.; Zhang, S.; Zou, C. Influence of pore water on the gas storage of organic-rich shale. *Energy Fuels* **2020**, *34*, 5293–5306. [[CrossRef](#)]
8. Schmidt, F.; Koch, B.P.; Goldhammer, T.; Elvert, M.; Witt, M.; Lin, Y.S.; Jenny, W.; Matthias, Z.; Verena, B.H.; Hinrichs, K.U. Unraveling signatures of biogeochemical processes and the depositional setting in the molecular composition of pore water DOM across different marine environments. *Geochim. Cosmochim. Acta* **2017**, *207*, 57–80. [[CrossRef](#)]
9. Fan, Q.; Cheng, P.; Tian, H.; Gai, H.; Xiao, X. Distribution and occurrence of pore water and retained oil in nanopores of marine-terrestrial transitional shales during oil generation and expulsion: Implications from a thermal simulation experiment on shale plug samples. *Mar. Pet. Geol.* **2023**, *150*, 106125. [[CrossRef](#)]
10. Li, J.; Wang, S.; Lu, S.; Zhang, P.; Cai, J.; Zhao, J.; Li, W. Microdistribution and mobility of water in gas shale: A theoretical and experimental study. *Mar. Pet. Geol.* **2019**, *102*, 496–507. [[CrossRef](#)]
11. Li, J.; Lu, S.; Zhang, P.; Li, W.; Jing, T.; Feng, W. Quantitative characterization and microscopic occurrence mechanism of pore water in shale matrix. *Acta Pet. Sin.* **2020**, *41*, 979–990.
12. Li, X.; Chen, S.; Wu, J.; Zhang, J.; Zhao, S.; Xia, Z.; Wang, Y.; Zhang, S.; Zhang, J. Microscopic occurrence and mobility mechanism of pore water in deep shale gas reservoirs: A typical case study of the Wufeng-Longmaxi Formation, Luzhou block, Sichuan Basin. *Mar. Pet. Geol.* **2023**, *151*, 106205. [[CrossRef](#)]

13. Li, X.; Chen, S.; Wang, Y.; Zhang, Y.; Wang, Y.; Wu, J.; Zhang, J.; Khan, J. Influence of pore structure particularity and pore water on the occurrence of deep shale gas: Wufeng–Longmaxi Formation, Luzhou Block, Sichuan Basin. *Nat. Resour. Res.* **2022**, *31*, 1403–1423. [[CrossRef](#)]
14. Ma, X.; Wang, H.; Zhou, S.; Feng, Z.; Liu, H.; Guo, W. Insights into NMR response characteristics of shales and its application in shale gas reservoir evaluation. *J. Nat. Gas Sci. Eng.* **2020**, *84*, 103674. [[CrossRef](#)]
15. Hanson, A.D.; Ritts, B.D.; Zinniker, D.; Moldowan, J.M.; Biffi, U. Upper Oligocene lacustrine source rocks and petroleum systems of the northern Qaidam basin, northwest China. *AAPG Bull.* **2001**, *85*, 601–619.
16. Dang, Y.; Zhao, W.; Su, A.; Zhang, S.; Li, M.; Guan, Z.; Ma, D.; Chen, X.; Shuai, Y.; Wang, H.; et al. Biogenic gas systems in eastern Qaidam Basin. *Mar. Pet. Geol.* **2008**, *25*, 344–356. [[CrossRef](#)]
17. Guo, Y.; Cao, J.; Liu, R.; Wang, H.; Zhang, H. Hydrocarbon accumulation and alteration of the Upper Carboniferous Keluke Formation in the eastern Qaidam Basin: Insights from fluid inclusion and basin modeling. *J. Pet. Sci. Eng.* **2022**, *211*, 110116. [[CrossRef](#)]
18. Wu, C.; Wu, D.; Mattinson, C.; Lei, M.; Chen, H. Petrogenesis of granitoids in the Wulan area: Magmatic activity and tectonic evolution in the North Qaidam, NW China. *Gondwana Res.* **2019**, *67*, 147–171. [[CrossRef](#)]
19. Wu, Y.; Liu, C.; Liu, Y.; Gong, H.; Awan, R.S.; Li, G.; Zang, Q. Geochemical characteristics and the organic matter enrichment of the Upper Ordovician Tanjianshan Group, Qaidam Basin, China. *J. Pet. Sci. Eng.* **2022**, *208*, 109383. [[CrossRef](#)]
20. Heermance, R.V.; Pullen, A.; Kapp, P.; Garzzone, C.N.; Bogue, S.; Ding, L.; Song, P. Climatic and tectonic controls on sedimentation and erosion during the Pliocene–Quaternary in the Qaidam Basin (China). *GSA Bull.* **2013**, *125*, 833–856. [[CrossRef](#)]
21. Owen, L.A.; Finkel, R.C.; Haizhou, M.; Barnard, P.L. Late Quaternary landscape evolution in the Kunlun Mountains and Qaidam Basin, Northern Tibet: A framework for examining the links between glaciation, lake level changes and alluvial fan formation. *Quatern. Int.* **2006**, *154*, 73–86. [[CrossRef](#)]
22. Kezao, C.; Bowler, J.M. Late Pleistocene evolution of salt lakes in the Qaidam basin, Qinghai province, China. *Palaeogeogr. Palaeoclimatol. Palaeoecol.* **1986**, *54*, 87–104. [[CrossRef](#)]
23. Zhao, Y.; Yu, Z.; Chen, F.; Ito, E.; Zhao, C. Holocene vegetation and climate history at Hurlig Lake in the Qaidam Basin, northwest China. *Rev. Palaeobot. Palynol.* **2007**, *145*, 275–288. [[CrossRef](#)]
24. He, S.; Tang, X.; Shao, Z.; Jiang, Z.; Wang, B.; Liu, X.; Wang, Y.; Xu, M. Pore Structure Characteristics, Genesis, and Its Controlling Effect on Gas Migration of Quaternary Mudstone Reservoir in Qaidam Basin. *Geofluids* **2022**, *2022*, 7098409. [[CrossRef](#)]
25. Zhang, M.; Dai, S.; Pan, S.; Jing, Z.; Wu, Z.; Chen, Y.; Du, B.; Zhang, J.; Liu, G.; Jiaoba, D.; et al. Deciphering the laminated botryococcus-dominated shales in saline lacustrine basin, Western Qaidam Basin, NW China: Implications for shale oil potential. *Mar. Pet. Geol.* **2023**, *155*, 106397. [[CrossRef](#)]
26. Li, Y.; Li, X.; Wang, Y.; Yu, Q. Effects of composition and pore structure on the reservoir gas capacity of Carboniferous shale from Qaidam Basin, China. *Mar. Pet. Geol.* **2015**, *62*, 44–57.
27. Visco, G.; Campanella, L.; Nobili, V. Organic carbons and TOC in waters: An overview of the international norm for its measurements. *Microchem. J.* **2005**, *79*, 185–191. [[CrossRef](#)]
28. Bhargava, S.; Awaja, F.; Subasinghe, N.D. Characterisation of some Australian oil shale using thermal, X-ray and IR techniques. *Fuel* **2005**, *84*, 707–715. [[CrossRef](#)]
29. Zhou, S.; Dong, D.; Zhang, J.; Zou, C.; Tian, C.; Rui, Y.; Liu, D.; Jiao, P. Optimization of key parameters for porosity measurement of shale gas reservoirs. *Nat. Gas Ind. B* **2021**, *8*, 455–463. [[CrossRef](#)]
30. Siddiqui, M.A.Q.; Ali, S.; Fei, H.; Roshan, H. Current understanding of shale wettability: A review on contact angle measurements. *Earth-Sci. Rev.* **2018**, *181*, 1–11. [[CrossRef](#)]
31. Yang, R.; Liu, W.; Meng, L. Multifractal Analysis of the Structure of Organic and Inorganic Shale Pores Using Nuclear Magnetic Resonance (NMR) Measurement. *J. Mar. Sci. Eng.* **2023**, *11*, 752. [[CrossRef](#)]
32. Miao, F.; Wu, D.; Liu, X.; Xiao, X.; Zhai, W.; Geng, Y. Methane adsorption on shale under in situ conditions: Gas-in-place estimation considering in situ stress. *Fuel* **2022**, *308*, 121991. [[CrossRef](#)]
33. Wang, Y.; Wang, X.; Song, G.; Liu, H.; Zhu, D.; Zhu, D.; Ding, J.; Yang, W.; Yin, Y.; Zhang, S.; et al. Genetic connection between mud shale lithofacies and shale oil enrichment in Jiyang Depression, Bohai Bay Basin. *Petrol. Explor. Dev.* **2016**, *43*, 759–768. [[CrossRef](#)]
34. Bradshaw, M.J.; Penney, S.R. A cored Jurassic sequence from north Lincolnshire, England: Stratigraphy, facies analysis and regional context. *Geol. Mag.* **1982**, *119*, 113–134. [[CrossRef](#)]
35. Jiang, Z.; Tang, X.; Cheng, L.; Li, Z.; Zhang, Y.; Bai, Y.; Yuan, Y.; Hao, J. Characterization and origin of the Silurian Wufeng–Longmaxi Formation shale multiscale heterogeneity in southeastern Sichuan Basin, China. *Interpretation* **2015**, *3*, SJ61–SJ74. [[CrossRef](#)]
36. Zou, C.; Dong, D.; Wang, Y.; Li, X.; Huang, J.; Wang, S.; Guan, Q.; Zhang, C.; Wang, H.; Liu, H.; et al. Shale gas in China: Characteristics, challenges and prospects (I). *Petrol. Explor. Dev.* **2015**, *42*, 753–767. [[CrossRef](#)]
37. AlRatrouf, A.; Blunt, M.J.; Bijeljic, B. Wettability in complex porous materials, the mixed-wet state, and its relationship to surface roughness. *Proc. Natl. Acad. Sci. USA* **2018**, *115*, 8901–8906. [[CrossRef](#)]
38. Zhao, T.; Jiang, L. Contact angle measurement of natural materials. *Colloids Surface. B* **2018**, *161*, 324–330. [[CrossRef](#)]
39. Schrader, M.E.; Yariv, S. Wettability of clay minerals. *J. Colloid Interf. Sci.* **1990**, *136*, 85–94. [[CrossRef](#)]

40. Yang, S.; Yu, Q. Experimental investigation on the movability of water in shale nanopores: A case study of Carboniferous shale from the Qaidam Basin, China. *Water. Resour. Res.* **2020**, *56*, e2019WR026973. [[CrossRef](#)]
41. Gao, H.; Cheng, P.; Wu, W.; Liu, S.; Luo, C.; Li, T.; Zhong, K.; Tian, H. Pore water and its influences on the nanopore structures of deep Longmaxi shales in the Luzhou block of the southern Sichuan Basin, China. *Energies* **2022**, *15*, 4053. [[CrossRef](#)]
42. Feng, D.; Li, X.; Wang, X.; Li, J.; Sun, F.; Sun, Z.; Zhang, T.; Li, P.; Chen, Y.; Zhang, X. Water adsorption and its impact on the pore structure characteristics of shale clay. *Appl. Clay. Sci.* **2018**, *155*, 126–138. [[CrossRef](#)]
43. Ning, Z.; Xu, B.; Zhong, W.; Liu, C.; Qin, X.; Feng, W.; Zhu, L. Preparation of phosphoric acid modified antibiotic mycelial residues biochar: Loading of nano zero-valent iron and promotion on biogas production. *Bioresour. Technol.* **2022**, *348*, 126801. [[CrossRef](#)] [[PubMed](#)]
44. Pan, Y.; Zhu, T.; He, Z. Minimizing effects of chloride and calcium towards enhanced nutrient recovery from sidestream centrate in a decoupled electrodialysis driven by solar energy. *J. Clean. Prod.* **2020**, *263*, 121419. [[CrossRef](#)]
45. McLatchey, G.P.; Reddy, K.R. Regulation of organic matter decomposition and nutrient release in a wetland soil. *J. Environ. Qual.* **1998**, *27*, 1268–1274. [[CrossRef](#)]
46. Hu, C.; Wang, F.; Liu, Y.; Zhi, J. Three-dimensional Lattice Boltzmann simulation of gas-water transport in tight sandstone porous media: Influence of microscopic surface forces. *Energy Sci. Eng.* **2020**, *8*, 1924–1940. [[CrossRef](#)]
47. Yang, Z.; Tang, X.; Xiao, H.; Zhang, F.; Jiang, Z.; Liu, G. Water film thickness of tight reservoir in Fuyu oil layer of Cretaceous Quantou Formation in Songliao Basin and its influence on the lower limit of seepage. *Mar. Pet. Geol.* **2022**, *139*, 105592. [[CrossRef](#)]
48. Liu, H.; Guo, W.; Fang, C.; Wang, H. A study on geological characteristics of marine shale gas reservoir in Southern China. *Energ. Explor. Exploit.* **2015**, *33*, 299–308. [[CrossRef](#)]
49. Zhang, T.; Ellis, G.S.; Ruppel, S.C.; Milliken, K.; Yang, R. Effect of organic-matter type and thermal maturity on methane adsorption in shale-gas systems. *Org. Geochem.* **2012**, *47*, 120–131. [[CrossRef](#)]
50. Chen, L.; Jiang, Z.; Jiang, S.; Guo, S.; Tan, J. Effect of pre-adsorbed water on methane adsorption capacity in shale-gas systems. *Front. Earth Sci.* **2021**, *9*, 757705. [[CrossRef](#)]
51. Zeng, Q.; Wang, Z.; McPherson, B.J.; McLennan, J.D. Modeling competitive adsorption between methane and water on coals. *Energy Fuel* **2017**, *31*, 10775–10786. [[CrossRef](#)]
52. Tian, H.; Wei, C.; Lai, Y.; Chen, P. Quantification of water content during freeze–thaw cycles: A nuclear magnetic resonance based method. *Vadose Zone J.* **2018**, *17*, 1–12. [[CrossRef](#)]
53. Eveline, V.F.; Akkutlu, I.Y.; Moridis, G.J. Numerical simulation of hydraulic fracturing water effects on shale gas permeability alteration. *Transp. Porous Med.* **2017**, *116*, 727–752. [[CrossRef](#)]

Disclaimer/Publisher’s Note: The statements, opinions and data contained in all publications are solely those of the individual author(s) and contributor(s) and not of MDPI and/or the editor(s). MDPI and/or the editor(s) disclaim responsibility for any injury to people or property resulting from any ideas, methods, instructions or products referred to in the content.